Supporting Information

Atomically precise chiral Ag_6 nanoclusters based on non-chiral ligands for acid/base stimulated luminescence response

Shuaibo Wang,[a] Weimiao He,[a] Yujia Cui,[a] Zhan Zhou,[a,b,*] Lufang Ma,[a,b] Shuang-Quan Zang[a,*]

[a]College of Chemistry, Zhengzhou University, Zhengzhou 450001, China

[b]College of Chemistry and Chemical Engineering, Henan Key Laboratory of Function-Oriented Porous Materials, Luoyang Normal University, Luoyang, 471934, China

*Corresponding author. Email: zhouzhan@lynu.edu.cn; zangsqzg@zzu.edu.cn

Crystallographic data collection and structural refinement: Single-crystal X-ray diffraction measurements of **Ag_6-*Rac***, **Ag_6-*S*** and **Ag_6-*R*** were performed on a Rigaku XtaLAB Pro diffractometer with Cu-Kα radiation (λ =1.54184 A) at 200/150 K. Data collection and reduction were performed using the program *CrysAlisPro*[1,2]. All the structures were solved with direct methods (*SHELXS*)[3] and refined by full-matrix least-squares on F^2 using *OLEX2*[4], which utilizes the *SHELXL2015* module[5]. All atoms are anisotropically refined, and the hydrogen atoms are placed at calculated positions in the ideal geometry and assigned fixed isotropic displacement parameters. There was a large solvent-accessible void volume in the crystals of **Ag_6-*Rac***, **Ag_6-*S*** and **Ag_6-*R***, which were occupied by highly disordered solvent molecules. The disordered solvent molecules in the structure could not be well identified, so the 'Solvent Mask' was adopted to remove them during structural refinement. The detailed information of the crystal data and refinement results for three compounds are summarized in Supplementary Table S1.

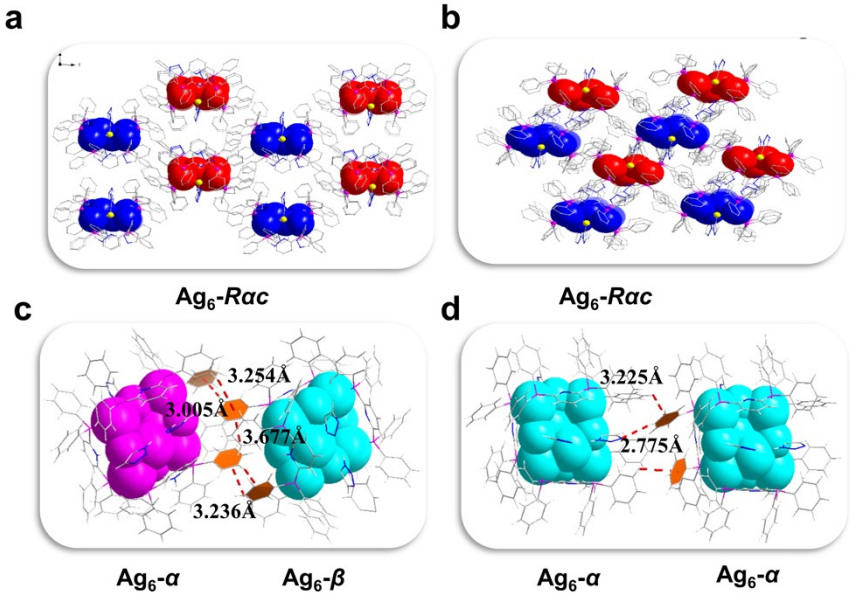

Figure S1. Packing of enantiomers in the lattice of **Ag_6-*Rac***. (a, b) Packing structures viewed along the b and c axis. (c) Intercluster weak interactions in the same layer. (d) Intercluster weak interactions between neighboring layers. Color labels: green, blue, red, Ag; yellow, S; pink, P; gray, C; light blue, N; light gray, H. Red dashed lines indicate the week interaction.

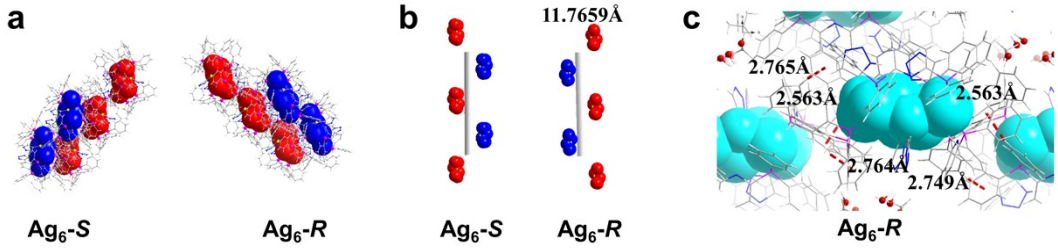

Figure S2. Cluster structure analysis diagram. (a) Spiral stacking figure of **Ag_6-*S*, Ag_6-*R***. (b) Smaller helix surrounding the helical tubes. (c) Weak intercluster forces.Color labels: blue, red, Ag; gray, C; light gray, H. Green dashed lines indicate the week interaction.

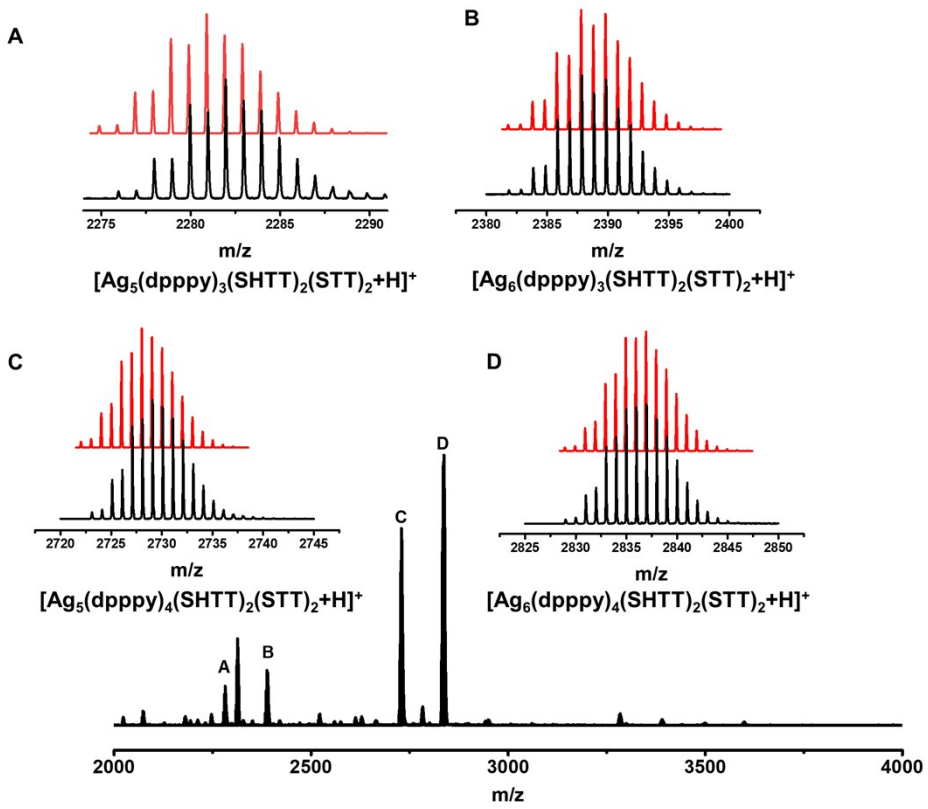

Figure S3. Mass spectra of racemic conglomerate **Ag$_6$-*S*/*R***.

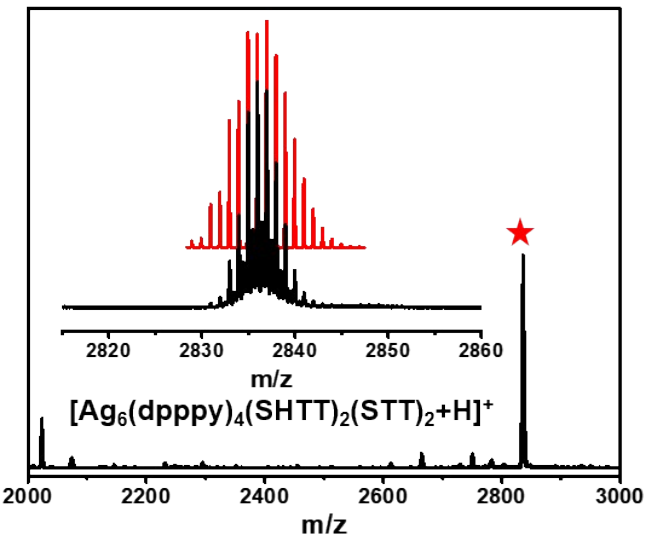

Figure S4. Mass spectra of **Ag$_6$-*Rac***.

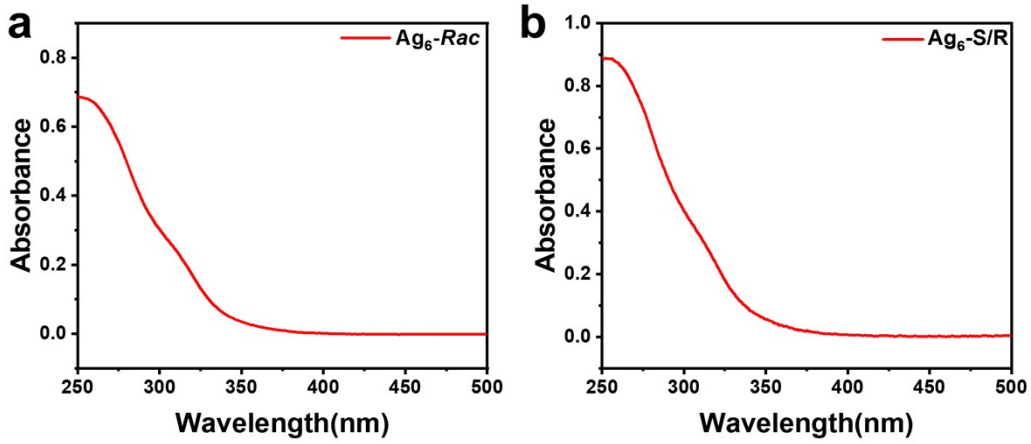

Figure S5. UV-Vis spectra of (a) **Ag_6-*Rac*** and (b) **Ag_6-*S*/*R***.

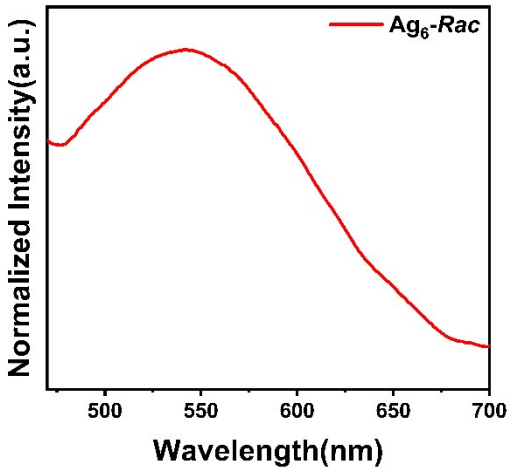

Figure S6. Fluorescence emission spectrum (λ_{ex} = 365 nm) of **Ag_6-*Rac*** in solid state.

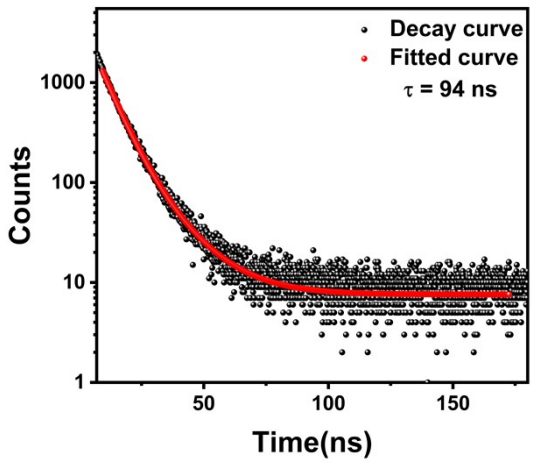

Figure S7. Temperature-dependent fluorescence decays of **Ag_6-*Rac*** in solid state.

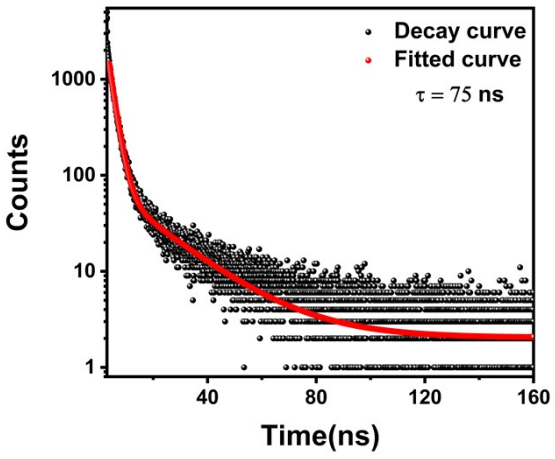

Figure S8. Temperature-dependent fluorescence decays of **Ag_6-*S*/*R*** solid (freshly prepared crystals).

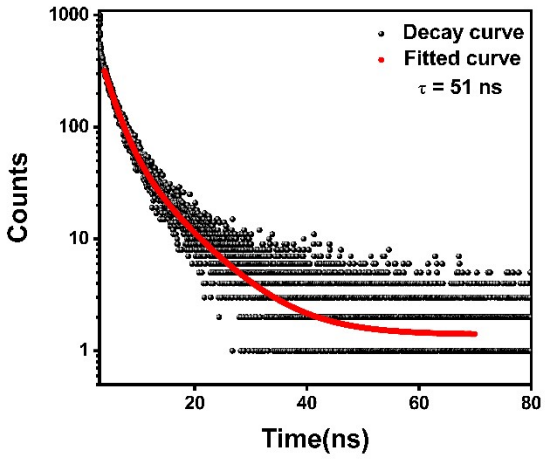

Figure S9. Temperature-dependent fluorescence decays of dry **Ag_6-*S*/*R*** solids.

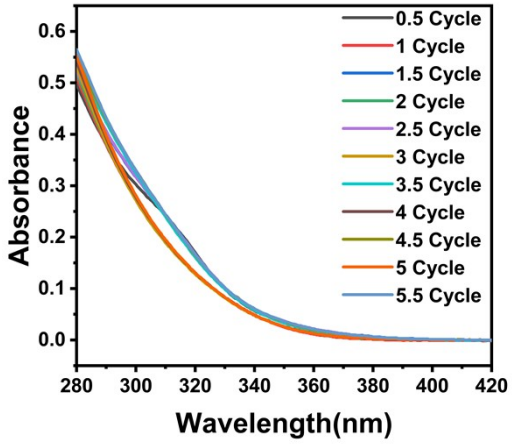

Figure S10. UV/Vis absorption spectrum of **Ag_6-*Rac*** on acid-base stimulation response.

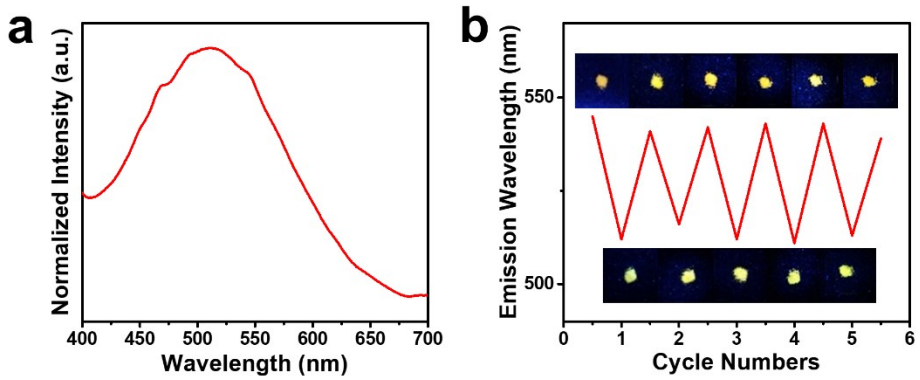

Figure S11. (a) Fluorescence emission diagram (λ_{ex} = 365 nm) of **Ag_6-*Rac*** in solid state under acidic environment. (b) Recycle diagram of **Ag_6-*Rac*** cluster at different emission wavelength (545 and 512 nm) with the fumigate by TFA or DEA. (Inset: Fluorescence photos of **Ag_6-*Rac*** solid were treated by (top) TFA and (below) DEA)

Compound	**Ag_6-*R***	**Ag_6-*S***	**Ag_6-*Rac***
CCDC number	2211323	2211324	2211325
Empirical formula	$C_{124}H_{98}Ag_6N_{16}P_8S_4$	$C_{124}H_{98}Ag_6N_{16}P_8S_4$	$C_{124}H_{102}Ag_6N_{16}O_2P_8S_4$
Formula weight	2835.40	2835.40	2866.04
Temperature/K	150.00	150.00	200.00
Crystal system	orthorhombic	orthorhombic	triclinic
Space group	$P2_12_12_1$	$P2_12_12_1$	P-1
a/Å	24.05180(10)	24.01420(10)	14.4279(2)
b/Å	24.08610(10)	24.14150(10)	17.4914(3)
c/Å	24.12200(10)	24.1607(2)	26.3185(4)
α/°	90	90	94.0460(10)
β/°	90	90	91.3660(10)
γ/°	90	90	109.9500(10)
Volume/Å^3	13974.21(10)	14006.90(14)	6219.58(17)
Z	4	4	2
ρ_{calc}/g cm^{-3}	1.348	1.345	1.530
μ/mm^{-1}	8.418	8.399	9.415
F(000)	5680.0	5680.0	2875.0
Crystal size/mm^3	0.12 × 0.09 × 0.07	0.12× 0.11 × 0.08	0.14 × 0.12 × 0.1
Radiation	Cu Kα (λ = 1.54184)	Cu Kα (λ = 1.54184)	Cu Kα (λ = 1.54184)
2θ range for data collection/°	5.184 to 149.204	5.174 to 149.55	5.394 to 130.998
Index ranges	-29 ≤ h ≤ 30, -30 ≤ k ≤ 29, -30 ≤ l ≤ 29	29 ≤ h ≤ 29, -30 ≤ k ≤ 30, -28 ≤ l ≤ 29	-17 ≤ h ≤ 17, -20 ≤ k ≤ 17, -26 ≤ l ≤ 31
Reflections collected	351767	33960	65292
Independent reflections	28438 [R_{int} = 0.0558, R_{sigma} = 0.0231]	28183 [R_{int} = 0.1031, R_{sigma} = 0.0409]	21270 [R_{int} = 0.0684, R_{sigma} = 0.0800]
Data/restraints/parameters	28438/0/1424	28196/0/1424	21270/104/1504
Goodness-of-fit on F^2	1.040	1.029	1.062
Final R indexes [I>=2σ (I)]	R_1 = 0.0369, wR_2 = 0.0983	R_1 = 0.0415, wR_2 = 0.1176	R_1 = 0.0628, wR_2 = 0.1451
Final R indexes [all data]	R_1 = 0.0388, wR_2 = 0.0994	R_1 = 0.0462, wR_2 = 0.1194	R_1 = 0.0934, wR_2 = 0.1564
Flack parameter	-0.0088(18)	-0.006(2)	

Table S1. Crystallographic data and structure refinement.

$R_1 = \sum||F_o|-|F_c||/\sum|F_o|$. $wR_2 = [\sum w(F_o^2-F_c^2)^2/\sum w(F_o^2)^2]^{1/2}$

Table S2 The main bond lengths (Å) for Ag_6-*R*.

Atom	Atom	Length/Å
Ag3	Ag4	3.0736(7)
Ag3	Ag2	3.0363(6)
Ag3	P4	2.4591(15)
Ag3	S4	2.6034(14)
Ag3	P3	2.4555(14)
Ag3	S1	2.7049(15)
Ag1	Ag2	2.9661(7)
Ag1	P8	2.4422(15)
Ag1	S4	2.6169(14)
Ag1	P2	2.4450(15)
Ag1	S3	2.7764(17)
Ag6	Ag4	2.8807(7)
Ag6	P5	2.4527(15)
Ag6	S2	2.7899(16)
Ag6	P6	2.4406(15)
Ag6	S1	2.6951(15)
Ag5	S2	2.7221(16)
Ag5	P1	2.5155(16)
Ag5	P7	2.5162(15)
Ag5	S3	2.7429(17)
Ag4	Ag2	2.8527(7)
Ag4	S2	2.5894(17)
Ag4	S1	2.4937(16)
Ag4	N11	2.185(5)
Ag2	S4	2.5871(16)
Ag2	S3	2.5296(18)
Ag2	N8	2.237(5)

Table S3 The main bond lengths (Å) for Ag_6-*S*.

Atom	Atom	Length/Å
Ag3	Ag4	3.0851(7)
Ag3	Ag2	3.0383(7)
Ag3	S2	2.6016(16)
Ag3	P1	2.4555(17)
Ag3	P2	2.4555(18)
Ag3	S3	2.6959(17)
Ag1	Ag2	2.9499(8)
Ag1	P3	2.4450(17)
Ag1	S2	2.6172(15)
Ag1	P4	2.4467(18)
Ag1	S1	2.768(2)
Ag6	Ag4	2.8815(7)
Ag6	P8	2.4525(18)
Ag6	S4	2.7785(18)
Ag6	P7	2.4433(18)
Ag6	S3	2.6984(17)
Ag5	P6	2.5165(18)
Ag5	S4	2.7221(18)
Ag5	P5	2.5167(18)
Ag5	S1	2.750(2)
Ag4	Ag2	2.8442(9)
Ag4	S4	2.5853(19)
Ag4	S3	2.4941(19)
Ag4	N11	2.186(6)
Ag2	S2	2.5894(19)
Ag2	S1	2.531(2)
Ag2	N5	2.243(7)

Reference

[1] CrysAlisPro, Version 1.171.36.31, Software for Crystal Data Collection and Reduction, Agilent technologies Inc., Santa Clara, CA, USA, 2012.

[2] CrysAlisPro 1.171.38.41k (Rigaku Oxford Diffraction, 2015).

[3] G. M. Sheldrick, A short history of SHELX, Acta Cryst. A, 2008, 64, 112-122.

[4] O. V. Dolomanov, L. J. Bourhis, R. J. Gildea, J. A. Howard, H. Puschmann, OLEX2: a Complete Structure Solution, Refinement and Analysis Program, J. Appl. Cryst., 2009, 42, 339-341.

[5] G. Sheldrick, Crystal Structure Refinement with SHELXL, Acta Cryst. C, 2015, 71, 3-8.